Bulletin of Engineering Geology and the Environment (2025) 84:204
https://doi.org/10.1007/s10064-025-04218-x

ORIGINAL PAPER

Fully remote assessment of rockfall incidents based on crowdsourced imagery

Pavlos Asteriou[1] · **Dimitrios Zekkos**[2] · **John Manousakis**[3]

Received: 19 November 2024 / Accepted: 6 March 2025

Abstract
This paper presents a fully remote approach for the assessment of rockfall incidents that is based on leveraging data that become available online with the goal to develop three dimensional (3D) models, document in detail the rockfall trajectory immediately following the incident and conduct rockfall analyses fully remotely. Such an approach can reduce the effort necessary to collect data and learn from incidents. The approach is well suited following natural disasters, where a wealth of field performance data may become available online through social media platforms and local news media. The steps to implement this approach involve: datamining the internet for crowdsourced data and particularly Unmanned Aerial Vehicle (UAV) footage of the incident, reconstructing the site morphology in the three-dimensional space by applying the Structure-from-Motion method, extracting insights from the crowdsourced data and conducting three-dimensional rockfall trajectory back-analysis. We demonstrate the approach through two incidents that occurred in Greece, where different amounts of crowdsourced data became available. We evaluate the proposed approach, discuss its limitations and benefits, and provide insights based on these two incidents. This paper shows that in both cases, the proposed approach enabled the rapid extraction of critical, perishable insights such as block detachment positions, block size, and fragment distribution. Also, the proposed approach allowed for the collection of all the input necessary to conduct detailed three-dimensional trajectory analyses. This supports the creation of high-precision inventories of both past and future incidents. Implementing this approach can enhance risk assessment accuracy, and inform mitigation strategies. The proposed approach allows the evaluation of geohazards globally fully remotely and possibly without the need for on-site visits.

Keywords Rockfall assessment · Crowdsourced data · Structure-from-motion · 3D trajectory analysis

Introduction

Rockfalls have significant consequences on communities and infrastructure and therefore represent a major hazard, especially in mountainous areas and rocky coastlines. Preparedness against rockfall hazard involves the identification of the elements at risk. This is accomplished by evaluating the probability of rockfall events, the spatial probability and intensity of impacts on structures and human activities, their vulnerability, and the related expected costs for different mitigation scenarios (Agliardi et al. 2009; Wang et al. 2014; Obda et al. 2024). Trajectory characteristics (path direction and length, velocity, and height distribution along the rockfall path) are required to design effective mitigation measures. Key consideration for analysis and mitigation designs is the documentation of previous rockfalls. This documentation can be used for hazard assessment (Guzzetti et al. 2004; Pierson 1991; Saroglou et al. 2012) where critical rockfall source areas can be identified, and as a basis of comparison against modeled rockfall trajectories.

In recent years, significant innovations have been made in mapping, characterizing, and modeling rockfalls. In general, the trajectory of a falling block can be described by four motion types; first, is the aerial phase that is terminated with an impact on the slope surface. Following the impact, the block can either rebound and become airborne again, or alternatively remain in contact with the ground

✉ Pavlos Asteriou
pasterio@civil.duth.gr

[1] Argo-E Group, Department of Civil Engineering, Democritus University of Thrace, Xanthi, Greece

[2] Department of Civil and Environmental Engineering, University of California at Berkeley, Berkeley, CA, USA

[3] Argo-E Group, Athens, Greece

Published online: 20 March 2025

and slide or roll on the slope surface. Impact is the most difficult part of the trajectory to predict, due to the inherent randomness of the parameters involved. Key parameters are the strength, stiffness, roughness, and inclination of the ground materials on the slope, the strength, stiffness, mass and shape of the block, as well as the translational and rotational velocity, the collision angle and orientation of the block at impact (Labiouse and Heidenreich 2009). Recent studies on modelling impact have focused on laboratory scale tests (Asteriou et al. 2012; Asteriou and Tsiambaos 2018; Buzzi et al. 2012); in-situ tests (Giacomini et al. 2012; Ma et al. 2021; Prades-Valls et al. 2022; Spadari et al. 2012); and back-analysis of natural rockfall events (Noël et al. 2023; Paronuzzi 2009; Saroglou et al. 2018). Laboratory tests provide insights on the effect of specific parameters and in-situ tests are preferred when assessing risk at a specific site.

Back-analysis of rockfall events is of particular value as the phenomenon occurs in the natural environment without being affected by testing assumptions, simplifications, or scale effects. A typical back-analysis of a natural rockfall event comprises of a field survey followed by trajectory modeling. The field survey is conducted to collect site-specific information of the incident. Specifically, the detachment area, impact tracks, block size, and runout distance as well as the site conditions, that include topography, geology, and vegetation coverage. In the trajectory modeling stage, the site characteristics are modeled and simulations are performed using a trial-and-error process until the modeled path replicates the actual trajectory path.

In recent years, commercial rockfall simulation software has been integrated with 3D terrain models. In conjunction with advancements in 3D mapping, the resolution of the terrain used in simulations is drastically increased compared to the simplified slope geometry obtained by traditional surveying methods that were used in previous years and were paired with two-dimensional rockfall analysis software. The transition to 3D analysis allows the assessment of lateral dispersion. Lateral dispersion has been shown to be affected by topography and can be significant in certain cases (Asteriou and Tsiambaos 2016; Azzoni et al. 1995; Crosta and Agliardi 2004) but was difficult to assess in the past due to the limitations on computational power and the lack of reliable 3D terrain models. Recent advancements in rockfall modeling include the use of the discrete element method that is capable of modeling the fragmentation of the block (Chi et al. 2015; Wang and Tonon 2011; Zhao et al. 2017) while, more recently, 3D game-engine platforms have been used (Hao et al. 2021; Harrap et al. 2019; Ondercin 2016; Sala et al. 2019) that are capable to simulate efficiently rockfall events comprised of many fragments.

Terrestrial or aerial Light Detection and Ranging (LiDAR) as well as optical data collected from the ground or by Unmanned Aerial Vehicles (UAV) can be deployed to generate detailed 3D terrain models. These models can be used to identify rockfall hazard areas (Cirillo et al. 2024), document the evolution of rockfall incidents using successive scans of the same slope (Sala et al. 2019) and provide the topography for trajectory simulation (Manousakis et al. 2016; Saroglou et al. 2017, 2018; Zekkos et al. 2018). UAVs are affordable for conventional engineering geology and geotechnical engineering practice and are increasingly used in hazard assessment globally because they offer rapid, high-resolution data. Studies from diverse regions have shown the utility of such technologies in monitoring rockfall and landslide events, supporting hazard assessment and response (Stumpf et al. 2013; Westoby et al. 2012; Šašak et al. 2019; Cirillo et al. 2024). Their capabilities have improved so that high-quality imagery or footage are readily acquired by off-the-shelf UAVs. Moreover, due to the lower cost of acquiring and deploying UAVs, it is becoming increasingly common to find UAV footage on the internet and social media platforms. This is particularly relevant following disastrous events that draw public attention, including rockfall incidents.

Key to rockfall data collection is the timing of data collection, that should be as short as possible to collect perishable data following the rockfall event. Identifying source areas can be done more easily and is less time sensitive. Machine learning algorithms have been developed with the goal of automating the process of identifying potential rockfall sources and classifying hazard based on the terrain characteristics (Fanos and Pradhan 2018; Farmakis et al. 2022). However, other information, such as the rockfall path and especially the trajectory characteristics, such as rolling vs. the bouncing section of a rockfall path, as well as the number of bounce locations, becomes less discernible with time. Damage to vegetation and the terrain becomes less discernible as vegetation grows and precipitation erases evidence of the rockfall event. In the cases that infrastructure is affected, restoration works may start shortly after the event. Despite advances in technologies such as UAVs and LiDAR that were described earlier, there is still a cost associated with collecting field data (An et al. 2024).

Because gathering field information still requires human resources and the timing of deployment is critical, an alternative, or better yet, a complementary approach that forms the research hypothesis of this paper, is to leverage data that becomes available online for a specific event and use it to conduct analyses completely remotely. This is becoming increasingly relevant nowadays following natural disasters, because a wealth of field performance data is becoming available online by local residents, even before any field

deployment is planned and this information has proven truly valuable in prioritizing field deployment activities (Yu et al. 2018). For example, tweets posted on social media have been used to assess earthquake impact on people and infrastructure within minutes after the event (Zekkos et al. 2019), and for flood event management in both crisis response and preventive monitoring (De Albuquerque et al. 2015).

Several initiatives have explored the use of crowdsourced data in geohazard studies, particularly in rockfall analysis. Zabota et al. (2020) developed a mobile application designed to compile an inventory of past rockfall events, demonstrating the potential of public engagement in geohazard documentation. Grady et al. (2024) utilized Google Earth imagery to create a detailed rockfall inventory for the Arequipa Region in Peru, highlighting the utility of readily available remote sensing data for regional-scale analysis. Jaud et al. (2022) integrated crowdsourced imagery into a geohazards observatory developed for the Giant's Causeway Coastal Cliffs in Northern Ireland. This approach enabled the generation of 3D models, facilitating the collection of larger volumes of data with improved spatial and temporal distribution, thus enhancing the monitoring and analysis of geohazards in the area. Recently, An et al. (2024) utilized UAV images obtained from live television broadcasts of the Xinjing landslide in China to reconstruct a 3D model of the affected area. They further analyzed the deformation using Particle Image Velocity (PIV) techniques, leveraging additional footage that captured the entire failure process. This innovative approach demonstrates the potential of integrating publicly available media with advanced analytical methods for geohazard assessment.

To evaluate this hypothesis, a fully remote approach to analyze rockfall incidents using exclusively crowdsourced optical data is presented. The approach leverages data that becomes available immediately following an incident and includes perishable information providing quick insights into the incident that can also be useful for immediate response and restoration decisions. Two rockfall incidents that occurred in Greece are presented and analyzed using data that was acquired by third-parties and became available online. Specifically, the first incident occurred on October 30, 2022, in Agia Fotia beach, near the city of Ierapetra in Crete, where a beach-side hotel was struck by a rock block and was severely damaged killing one tenant. The second occurred on December 1, 2022, in Kakia Skala area in Attica, where the main highway, which connects Athens with Corinth and more broadly the Western Greece and Peloponnese, was impacted by a block causing a temporary closure. We demonstrate and evaluate the methodology used, discuss the limitations and benefits associated with such an approach, and illustrate the insights gained from these two incidents.

Methodology

For both incidents presented and analyzed hereafter, UAV footage became available on social media within hours following the event and was widely broadcasted by local and national media on the same day. Figure 1 shows information on the incidents and on the media coverage.

Image frames were extracted from the UAV footages and the imagery was processed using the Structure from Motion (SfM) method so that 3D Point Clouds are developed for each case. The commercial software ContextCapture by Bentley was used in this study. As described in Manousakis et al. (2016), SfM combines the benefits of photogrammetry and computer vision to reconstruct a 3D scene by auto-identifying matching features, estimating their location, obtaining the relative location of the acquisition positions (i.e., location of the UAV when the photo was taken), and producing a sparse 3D point cloud of those features. Internal (camera focal length, image sensor format, principal point, lens distortion coefficients) are used as initial values and external camera calibration parameters (camera positions and orientations) are calculated and refined during the bundle adjustment phase.

There are several issues, or differences, associated with the fully remote approach implemented herein where the footage is collected from the public, compared to the collection of field data by professionals for the direct objective to analyze a rockfall incident. First, the footage may be collected along a flight path that is irregular and may lead to incomplete coverage of the target from different aspects. In both case studies presented herein, the footage was proven to be adequate and captured the entire failure area allowing for a 3D scene reconstruction. A second issue is that the internal camera parameters are not known, since the camera used for the footage is not reported. However, with adequate optical data (imagery frames), the algorithm converges and the internal camera parameters are back-calculated. Third, because the imagery is extracted from a video, there is no known positioning (e.g. GPS) of the imagery shown, and certainly not ground control points, which would normally be collected as part of such an expedition (Carvajal-Ramírez et al. 2016; Manousakis et al. 2016).

As a result, a global georeference for the 3D model cannot be immediately defined. Therefore, the model is reconstructed in a local positioning system. The scale of the model can be accurately established by measuring specific features of the scene in satellite imagery such as GoogleEarth and the vertical (gravitational) axis of the model can be defined from vertical features of the scene (e.g. the edges of the buildings). Subsequently, and possibly as an alternative approach, the 3D model can be pinned to a previously available 3D model of the same area that is properly scaled and

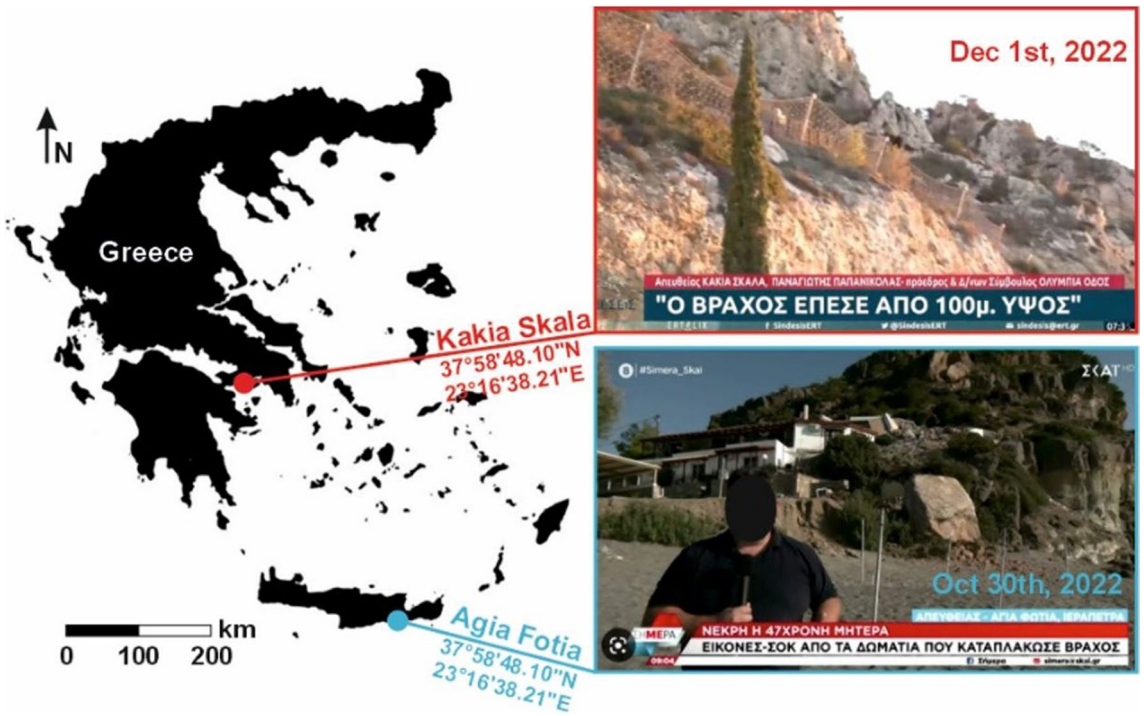

Fig. 1 Location (latitude and longitude) and media coverage snapshots of the two rockfall incidents (top: Kakia Skala (ert.gr); bottom: Agia Fotia (skai.gr)). Journalist's face edited for privacy reasons

georeferenced. For example, 3D models available from national mapping efforts or Cadastres, can be used for that purpose. Both approaches were conducted in this study.

Although the developed 3D models have high resolution and capture valuable information of the incident, it is important to have additional data prior to the event so that specific aspects of the event, such as the detachment source, the impact traces on the slope and the 3D terrain can be reliably attributed to that specific event. This information can also be provided by crowdsourced photos and videos collected prior to the event. Sources of imagery may include individuals posting images in GoogleEarth, GoogleMaps or similar applications. They can also be retrieved by datamining online digital maps. Crowdsourced UAV video footage that was collected for other purposes can also be found online, although it is still not as frequently available. More effort may be needed to detect such footage as it is not often embedded in digital maps. Overall, more populated areas have more online data available, increasing both the chances of identifying footage with the exact location of the incident and the redundancy of the data collected. It is important to also consider the timing of the footage, particularly the time elapsed between the pre- and post-rockfall data. Shorter elapsed times may provide more confidence that all observations in the post-event footage are relevant to that event, as opposed to previous events. Longer elapsed times and pre-event footage collected at different times may provide insights into the history of the site, the evolution of a rockfall detachment process, or possibly the occurrence of similar, possibly smaller events that were not noticed.

Crowdsourced photos and UAV video before the incidents were datamined online for both incidents. A YouTube© video of the Agia Fotia site before the incident had been generated and uploaded for tourist promotion purposes and was identified following the occurrence of the incident. The video was filmed on June 19, 2021, approximately 18 months before this incident. That footage is more recent to the failure than the nationwide topographic data that is dated 2007–2009 and is of 10 m resolution. A UAV footage of the Kakia Skala area before the incident was not publicly available despite the significant highway traffic because the area of Kakia Skala is a narrow and steep region without any developments nearby and no nearby traffic rest areas.

For each of the study sites, 3D models were generated using the available footage. To evaluate the proposed approach and the accuracy of the 3D terrain created from the crowdsourced data, the Digital Terrain Model (DTM) and its accompanying orthophoto were retrieved from the Hellenic Cadastre.

After generating a 3D surface model and collecting detailed documentation about the incident, a 3D trajectory back-analysis is performed using RocFall3 software (RocScience 2022). RocFall3 is a 3D statistical analysis program designed to determine the trajectory of the projectiles to

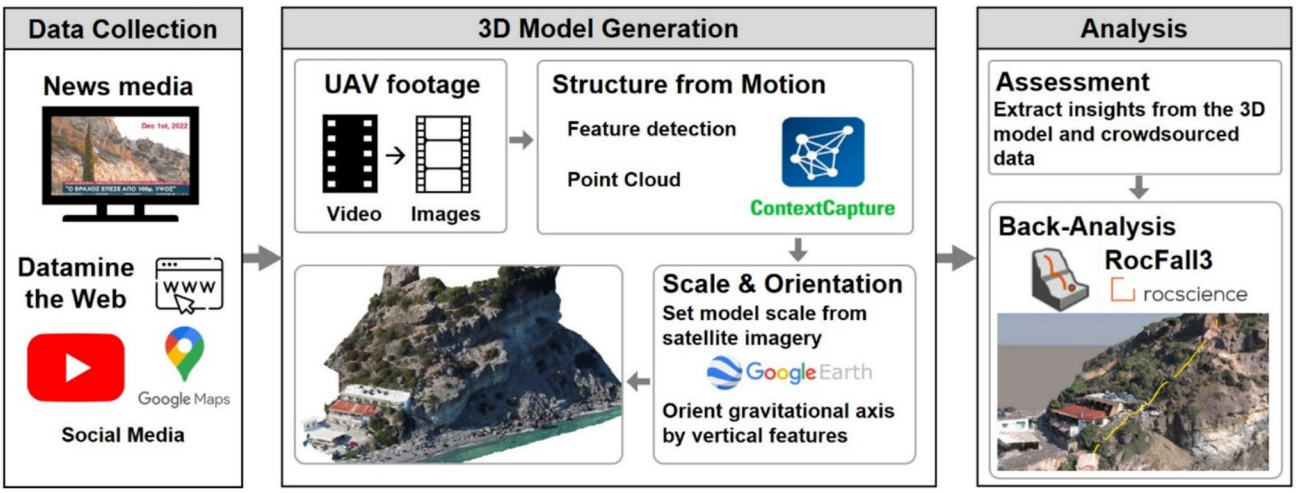

Fig. 2 Workflow illustrating the methodology used in this study, from disaster identification to 3D model generation and to the remote back-analysis of rockfall incidents

assess slopes at risk and design mitigation measures for rockfall. The objective of a back-analysis is to match the simulated trajectory with field observations and gain insights on what happened during the incident and derive material properties related to the rockfall that can be used in rockfall risk mitigation.

Figure 2 illustrates the workflow implemented in this study, providing a step-by-step visual of the process. The workflow begins with the identification of the disaster event and the collection of relevant data from the web. The next step is to generate the 3D model by extracting the frames from the collected videos, implementing the SfM method and scaling and orienting the 3D model. Finally, the 3D model is assessed to extract insights, and the 3D back-analysis is performed. Figure 2 also highlights the various software tools utilized at each stage of the process.

Agia Fotia rockfall incident

Agia Fotia setting

Agia Fotia is a settlement located in the southern part of the Lasithi region in Crete and serves as a tourist destination due to its large beach. The area comprises of sedimentary rocks of the Pliocene series and fluvial torrential deposits (Papastamatiou et al. 1959). Tectonically, the area is controlled by a primary fault system trending E-W and a secondary NW–SE system, which have contributed to the morphological shaping of the region.

The material at the detachment area is a thick-bedded conglomerate with a moderate degree of diagenesis, overlying primarily coarse sands and marls. The stratification dips toward the slope with an average inclination of 5° to 20°, while a vertical system of discontinuities is also identified.

Weathering of the rock, as well as wave action, results in marginally stable and overhanging blocks. Failures are frequent on the slope, as evidenced by the accumulation of rock debris on the base of the slope. The occurrence of the incident likely accelerated by heavy rainfall that impacted the area in the days leading up to the event.

3D model reconstruction

Two UAV video footages were found for the Agia Fotia site. The pre-incident footage was collected 18 months before the incident (https://rb.gy/5n6nvm) and the post-incident footage was filmed one day after the incident (https://www.youtube.com/watch?v=ArhPeJD-_PE). Both videos are FHD (full high definition) having a resolution of 1920×1080 pixels. Figure 3 presents the extracted video frame positions from the UAV footage in 3D space over the reconstructed 3D terrain, that were used in SfM method to reconstruct the pre- and post-incident 3D surface models. Both flights were conducted manually covering the area of interest from a variety of viewing distances and angles. The post-incident footage features also short range shots from various viewing angles. To achieve adequately high (> 80%) overlap between image frames and considering the video playback speed, frames were extracted every 1 s. In total, 468 frames were extracted and processed for the pre-incident model and 338 frames for the post-incident model.

The scaling of the 3D models was made by setting the distance of a well-defined horizontal feature of the scene as measured in GoogleEarth. The pre-incident 3D model covers an area of 2 km^2 (500 acres) and the post-incident 3D

Fig. 3 Extracted video frames positions from UAV footage in 3D space over reconstructed 3D terrain. (**a**) pre incident 3D model, (**b**) post-incident 3D model

model is 1.7 km^2 (420 acres). The estimated flight height for the pre-incident model, based on the scaling process, ranged between 50–80 m. This distance, along with the calculated camera internal parameters, results in an average ground resolution of 3 cm/pixel. For the post-incident 3D model, the flight height ranged between 3–40 m resulting in an average ground resolution of 2 cm/pixel. Oblique views of the 3D models are presented in Fig. 4a and b.

The post-incident model was subsequently used as reference for refining the registration and alignment of the pre-incident model through the equivalent point pairs alignment process that is available in CloudCompare. Eight point pairs were identified and the resulting root of the mean squared distances (RMS) 3D error was 21 cm. This is a reasonable error given the limitations imposed by the source data (video frames compared to structured high-resolution geolocated images and lack of GCPs), but is deemed adequate for the purposes of rockfall analyses. To further improve the registration of the two entities, we first implemented the Iterative Closest Point (ICP) registration algorithm within CloudCompare, which finely registers the two point clouds in an automatic process, and the resulting RMS 3D error was 5.2 cm with a standard deviation of 42 cm. The error in the vertical axis associated with the alignment of the two point clouds is estimated to be 4.0 cm with a standard deviation of 29 cm.

Evaluation of the 3D model

Reproducibility of the 3D model

The reproducibility of crowdsourced UAV data was assessed by comparing the two UAV-based 3D models. This was quantified using the Cloud-to-Cloud (C2C) distance calculation tool in CloudCompare, that allows the measurement of the nearest neighbor distance from points in one cloud to the other cloud. Figure 4c presents the point cloud comparison of the two models. The color scale indicates the signed distance between the two models which is calculated using a local model (2.5D triangulation) of the post-incident point cloud as the reference surface. Since the post-incident point cloud is dense enough, it approximates the normal distance from the pre-incident point cloud. Setting the pre-incident 3D model as the basis, blue (negative distances) indicates inward distance which corresponds to loss of volume, and red corresponds to outward distance, that represents a gain of volume.

An optical assessment of the data indicates that it is reasonable to assume that the observed major differences of the 3D models are attributed to the incident. The effects are discernible in Fig. 4c and highlighted in the boxes: Box (a) represents the detachment location, box (b) represents a block fragment, box (c) the damaged hotel room; and box (d) represents the block rest position.

The RMS is used as a metric of similarity with lower RMS representing a better match. Although there are not universally acceptable RMS values for all applications, by comparing the entire models, including areas of change due to the rockfall incident, the RMS is 5.2 cm with a standard deviation of 42 cm which is considered reasonable. When excluding the areas that have been affected by the rockfall and the objects that were moved in-between (numbered boxes in Fig. 4c), model differencing results in significantly lower RMS, equal to 1 cm with a 25 cm standard deviation.

Note that the point-cloud comparison presented in Fig. 4c includes vegetation. Removal of vegetation would result in more accurate 3D terrain models and would reduce differences between them. The vegetation on this site belongs to the species of Quercus Coccifera, that is a bush less than 2 m high with a thin stem (< 5 cm). Especially along the rock fall path, the vegetation is small compared to the size of the detached block and the overall geometry of the slope, and thus, vegetation removal was not considered necessary for the purposes of volume differencing and block size calculations, shown in Fig. 4c. Vegetation is also important in rockfall analyses as discussed subsequently. Removal of vegetation provides

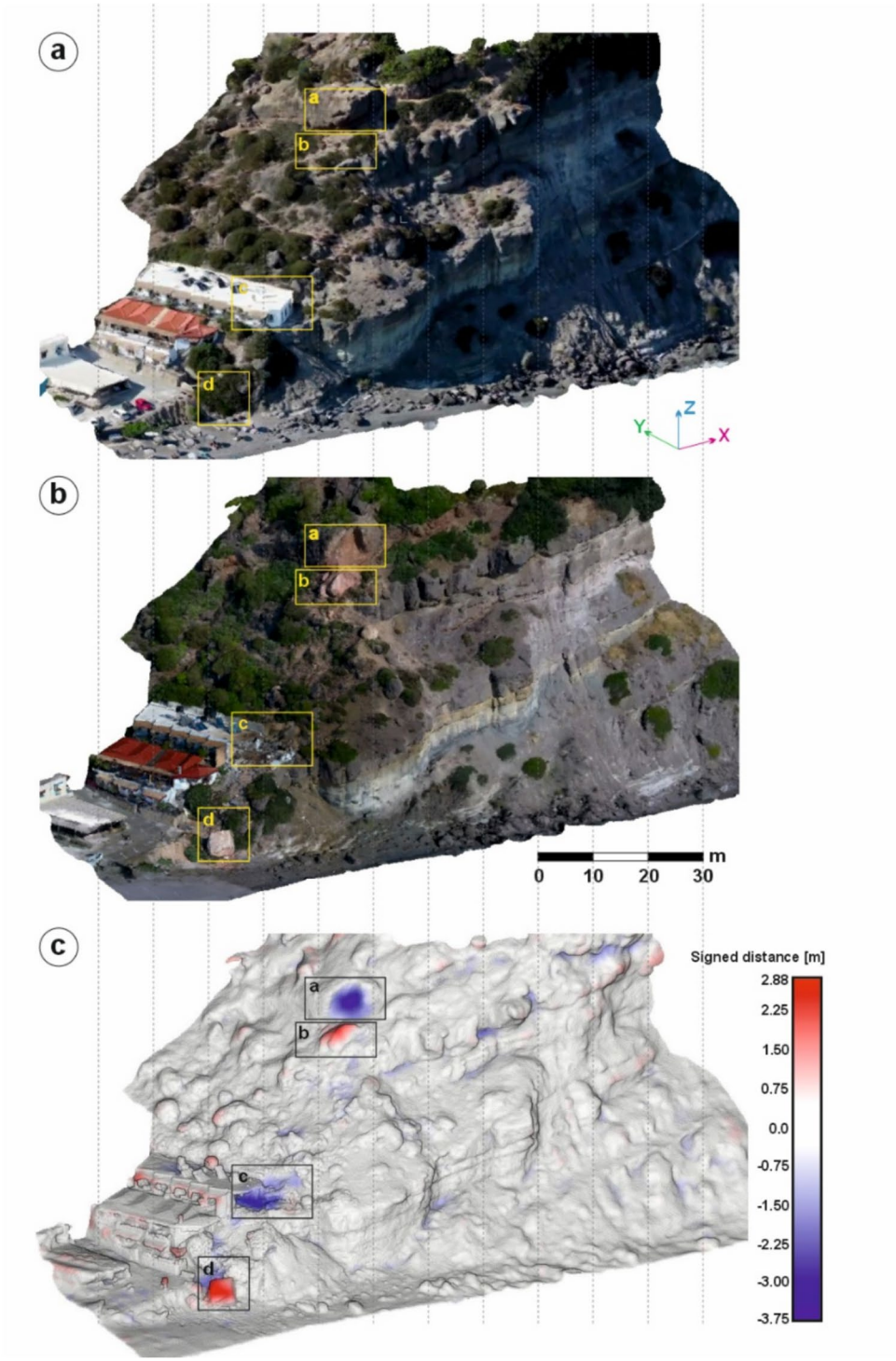

Fig. 4 Oblique views of the Agia Fotia 3D model; **a**. pre-incident, **b**. post-incident and **c**. point cloud comparison of the pre- and post-incident 3D models. Notable features include the detachment position (box a), a block fragment resting just below the detachment position (box b), the damage to the white building (box c), and the trajectory endpoint of the block that damaged the building (box d). In Fig. 4c. blue (negative distances) indicates inward distance, corresponding to material loss, and red represents outward distance, indicating material gain. The grey color covers 2 times the standard deviation (±0.42 m)

a better representation of ground terrain which is valuable. However, vegetation removal results in holes in the terrain model that are typically filled by interpolation between actual terrain points. Vegetation does influence the surface characteristics along the rockfall trajectory both for the rolling and the bounce aspects, and its presence increases energy dissipation (Dorren and Berger 2006) along the rockfall. However, in this case, since the vegetation comprises of low bushes and the detached block is of considerable size, the effect on energy dissipation due to the vegetation is small, according to the findings of Moos et al. (2017). Vegetation was partially removed for the rockfall analyses, as described subsequently, although it was not deemed that the specific vegetation along the path of the rockfall played a major role.

3D model Comparison with Cadastre

The 3D model generated was compared to the DTM model from the Hellenic Cadastre in an effort to validate the 3D models that were created (Fig. 5). The Cadastre is based on aerial photogrammetric methods using aerial photo strips and has a 10 m pixel size on the ground. The geometric accuracy of the DTM is RMSEz ≤ 2.0 m and the absolute accuracy is ≤3.92 m for a confidence level of 95%. This model is not considered a high resolution and accuracy model, and thus is not ideal for comparison with the high-resolution model that was developed, but represents a nationwide 3D model that can be used as a reference. DEMs with a high resolution (less than 5 m) are associated with high accuracy and detailed structural characteristics and are suitable for local-scale occurrences, while medium-resolution (from 20 m to 30 m) models illustrate the topographic features and are suitable for regional scale events (Kakavas and Nikolakopoulos 2021). The equivalent point distance resolution of the 3D model is approximately 5 cm. Because the 3D model area is small, the slope is steep and vegetated and the resolution of the models differ significantly, the comparison between the 3D model and the Hellenic Cadastre DTM results in an RMS of 176 cm with a standard deviation of 215 cm. This is considered a high RMS, and the differences can be attributed to the quite different resolution of the models as well as the presence of vegetation. However, as shown in Figure 5 the two models match in areas of bare rock. This indicates that the main morphological features match in form and scale between the two models. Therefore, the reconstruction process using the crowdsourced UAV footage is reliable.

The scale of the 3D model was also assessed using the Hellenic Cadastre orthophoto, which is orthorectified and adjusted to the Hellenic Cadastre DTM, allowing the measurement of true distances in the horizontal plane. The Hellenic Cadastre orthophoto has a 50 cm pixel size, the geometric accuracy is RMSExy ≤ 1.41 m and the absolute accuracy is ≤ 2.44 m for a confidence level of 95%. Figure 6 presents the Hellenic Cadastre orthophoto (a) and the plan view of the 3D model (b). The outline of the building across from the hotel is shown in yellow in both the 3D model and the orthophoto. We measured four reference distances on the horizontal plane (red lines in Figure 6a) in both the model and the orthophoto and calculated the mean error to be equal to 25cm. Given that the pixel size of the orthophoto is 50 cm, the error is well within the sub-pixel tolerance, confirming the correct scaling of the model.

In summary, the 3D models created using the crowdsourced data from different sources resulted in similar models, showing that the process is reproducible. The geometry of the slope is well defined and very similar to the Hellenic Cadastre DTM model and the scaling of the model is correct. This highlights that the 3D models created from crowdsourced data are reliable and can be used in event reconnaissance.

Rockfall assessment

The detachment position was determined by two different sources. First, by comparing crowdsourced images of the slope before and after the incident (Fig. 7), and second by comparing the two 3D models, before and after the incident,

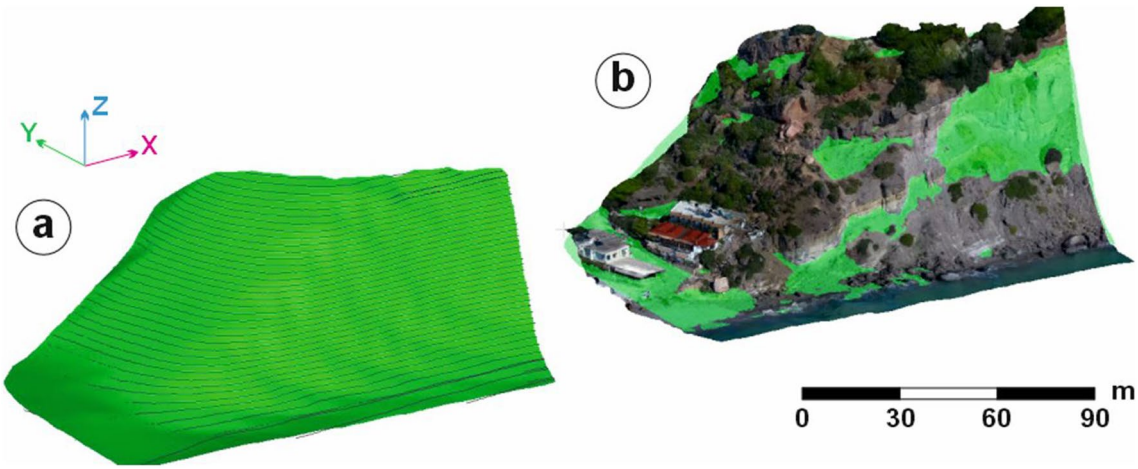

Fig. 5 Comparison of the 3D model generated was compared to the DTM model from the Hellenic Cadastre DTM **a**. surface shape according to the Hellenic Cadastre and **b**. Hellenic Cadastre DTM model superimposed in the generated 3D model from the UAV footage

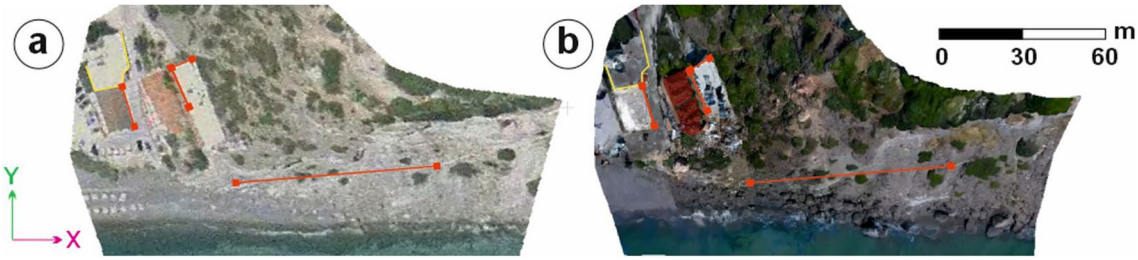

Fig. 6 Reference distances to evaluate the scaling of the 3D model in the Hellenic Cadastre orthophoto (**a**) and in the plan view of the 3D model (**b**)

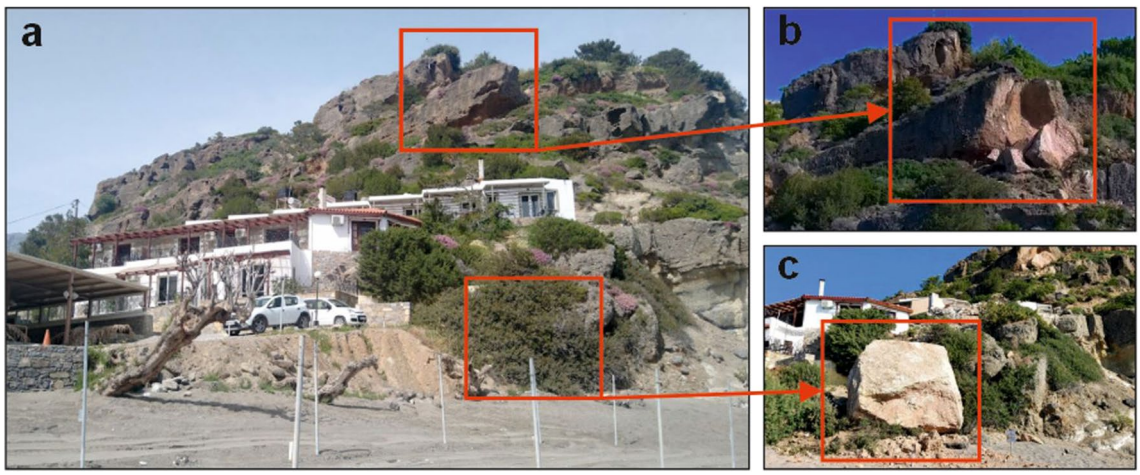

Fig. 7 Agia Fotia scenery before (**a**) and after (**b** & **c**) the rockfall (Image (**a**) was captured by T. Seifert on April 2022 and originates from google.maps; image (**b**) is extracted from the UAV video; and image (**c**) is retrieved from flashnews.gr – photo courtesy of M. Tsagaraki)

as presented earlier. Both methods resulted in the same detachment location.

By using the pre- and post-incident 3D models, not only the exact location, but also the detached volume is determined. This is done by superimposing the two 3D models and measuring their difference in the detachment location. This assumes that the observed difference is due to this incident, which based on visual inspection seems to be the case. Boolean operations in CAD software between 3D solids were used to calculate 3D volumes. Figure 8 shows this process, which resulted in a total detached volume of approximately 145 m^3 with a footprint of ~ 5 m x ~ 5 m and a height of ~ 6 m. Based on the estimated error of the point cloud alignment in the vertical direction (0.04 m), we estimate a volume uncertainty equal to 0.04 m × 5 m x 5m = 1 m^3 which represents less than 1% of the total detached volume, which is deemed small. Therefore, the accuracy of the models is appropriate for volume determination. Note that a large portion of the detached volume moved ~ 6 m and stopped, as seen Fig. 7b.

Through DEM differencing along the entire rockfall path, the positive volumes on the post-incident model can be used to calculate the size of the blocks. By comparing the 3D models, we estimate that the detached block

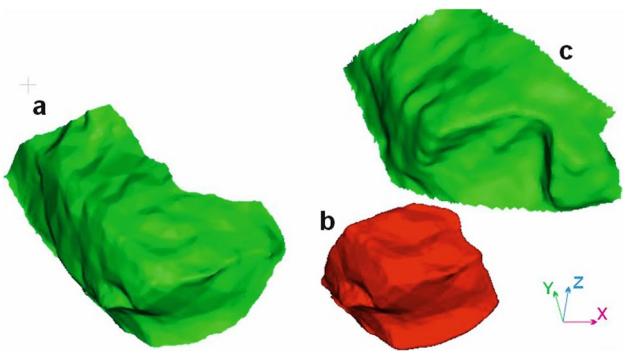

Fig. 8 Detached block position and size determination from the pre- and post-incident 3d models: a. pre-incident model, b. detached block; and c. post-incident model

fractured into at least four pieces of significant size ($> 1m^3$). Figure 9 shows these pieces scattered on the slope, which have an estimated total volume of ~ $134m^3$ ($V_1 = 51m^3$, $V_2 = 16.5m^3$, $V_3 = 1.5m^3$ and $V_4 = 65m^3$). The difference between the detached volume ($V = 145m^3$) and the volume of the four big pieces ($V = 134m^3$) can be attributed to broken pieces of size smaller then $1m^3$ that are scattered on the slope and are not identified in our analysis, blocks that were removed during the rescue operation, blocks that may have travelled beyond the extent of the model and possibly on the right side towards the sea, as well as potential volume calculation errors associated with DEM differencing.

At the path's endpoint the fallen block (V_4) resembles a rectangular prism, with a mass m = 162.5 T (assuming a density ρ of 2500 kg/m^3). That block (V_4) traveled a 3D distance of approximately 52 m and descended vertically 35 m where it reached the beach. The mean gradient of the slope at the rockfall path is approximately 42°.

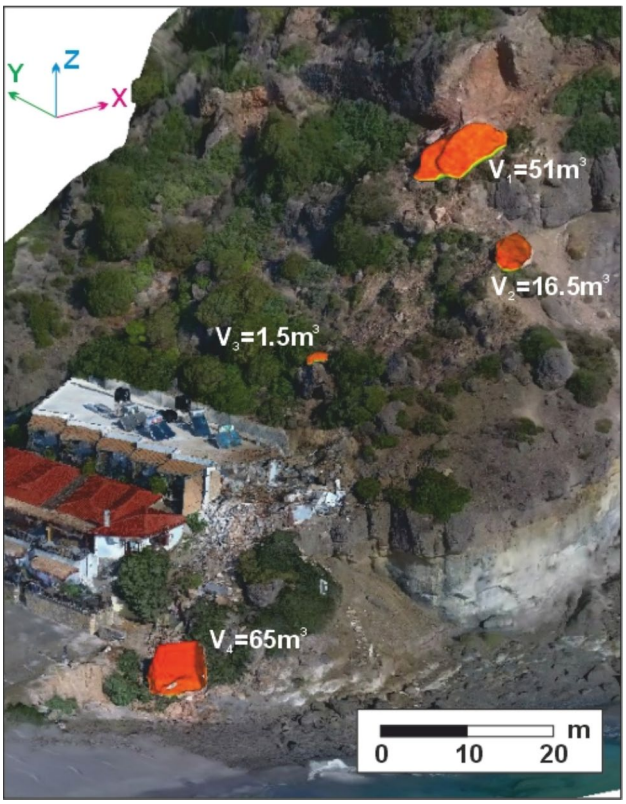

Fig. 9 Volume estimates of the block fragments scattered on the slope

Rockfall back-analysis through simulations

The back-analysis of this incident is performed using the lumped mass approach. In this method, each rock is modelled as an infinitesimal spherical particle, without size, but with mass used to calculate the kinetic energy. The parameters used for the analysis, which are the Coefficients of Restitution, and friction angle, are shown in Table 1 and were estimated based on the suggested values in relevant literature (Heidenreich 2004; Hoek 1987; Pfeiffer and Bowen 1989) and by the authors' experience in similar formations.

Using the lumped-mass model, the size and the shape of the block does not affect the trajectory paths, and the analysis cannot consider possible fracturing of the block during its fall. As mentioned earlier, a significant mass of the detached rock block, calculated equal to 54 m^3, traveled only a few meters before arresting. To overcome this limitation and estimate realistic kinetic energy at impact with the hotel, we assumed that the block mass at the detachment position was equal to the mass of block V_4, as measured at the trajectory endpoint. We recognize that this represents a limitation of the modeling effort in this paper and other approaches, such as DEM modeling (Chi et al. 2015; Wang and Tonon 2011; Zhao et al. 2017) or game-engine platforms (Hao et al. 2021; Harrap et al. 2019; Ondercin 2016; Sala et al. 2019) that consider block fracturing may be more appropriate.

The post-incident 3D terrain model was used for the trajectory analysis in RocFall3 software. Since the trajectories generated are affected by surface roughness, the 3D model was manually cleaned in order to remove the blocks right after the detachment position (Fig. 4 – box b). In addition, part of the vegetation that stood in the trajectory paths was also manually removed. The surface elements that were removed from the model resulted in holes on the model that were then filled with interpolated smooth triangles.

Since the release direction of the block cannot be deduced from the available data, an offset of ±30° with respect to the dip direction of the slope was assumed in order to cover all possible

Table 1 Parameters used in rockfall analysis

Parameter		Agia Fotia	Kakia Skala
Normal coefficient of Restitution	R_n [-]	0.30 ± 0.04	0.35 ± 0.04
Tangential coefficient of restitution	R_t [-]	0.85 ± 0.04	0.85 ± 0.04
Friction angle	φ [°]	15 ± 5	20 ± 5
Block volume	V [m^3]	65	1
Mass	m [T]	162.5	2.5

directions. Also, as the block detached under static conditions, a low initial translational velocity of 1 m/s was assigned to the block at the detachment position to initiate the fall. A total of 100 blocks were released from the detachment position, to allow for a statistically significant interpretation of the results.

Figure 10a presents the trajectory paths as calculated by RocFall3 software, where the color indicates the bounce height. Figure 10b illustrates the spatial distribution of the trajectory endpoints. Note that the actual path is replicated by 3% of the trajectories calculated by RocFall3. However, the hotel (dashed yellow rectangle in Fig. 10b) is affected by more than 50% of the simulated trajectories.

Lateral dispersion is defined as the ratio of the distance between the two extreme fall paths (as seen looking at the face of the slope) and the length of the slope (Azzoni and De Freitas 1995). The factors that control lateral dispersion can be grouped into three categories (Crosta and Agliardi 2004): macro-topography factors, related to the overall slope geometry; micro-topography factors, controlled by local roughness of the slope; and dynamic factors, associated with the interaction between slope features and block dynamics during bouncing and rolling. Experimental results (Azzoni and De Freitas 1995) indicate that dispersion is generally in the range of 10–20%, regardless of the length of the slope, and steeper slopes produced a smaller dispersion. Based on the rockfall paths calculated by RocFall3, lateral dispersion is 64.2%. This is considerably higher compared to the findings of Azzoni and De Freitas (1995), yet anticipated at a convex topography where the block can deflect significantly.

Fig. 11 Oblique view of the closest rockfall trajectory obtained from RocFall3 back-calculations superimposed on the 3D digital model

Figure 11 illustrates the simulation that most closely resembles the actual rockfall path, superimposed on the digital model. The evidence is showing that the actual trajectory is well simulated by the closest trajectory and specifically:

i. Visible traces of sliding are seen on the actual site on the top part of the slope. This is well replicated by the trajectory calculated by RocFall3, as the simulation also indicates a sliding motion type.
ii. No impact or sliding traces are visible in the proximity of the hotel in the upslope direction, indicating that the block was airborne and landed onto the hotel room. This is also consistent with the magnitude of the damage and the scatter of the debris. In the simu-

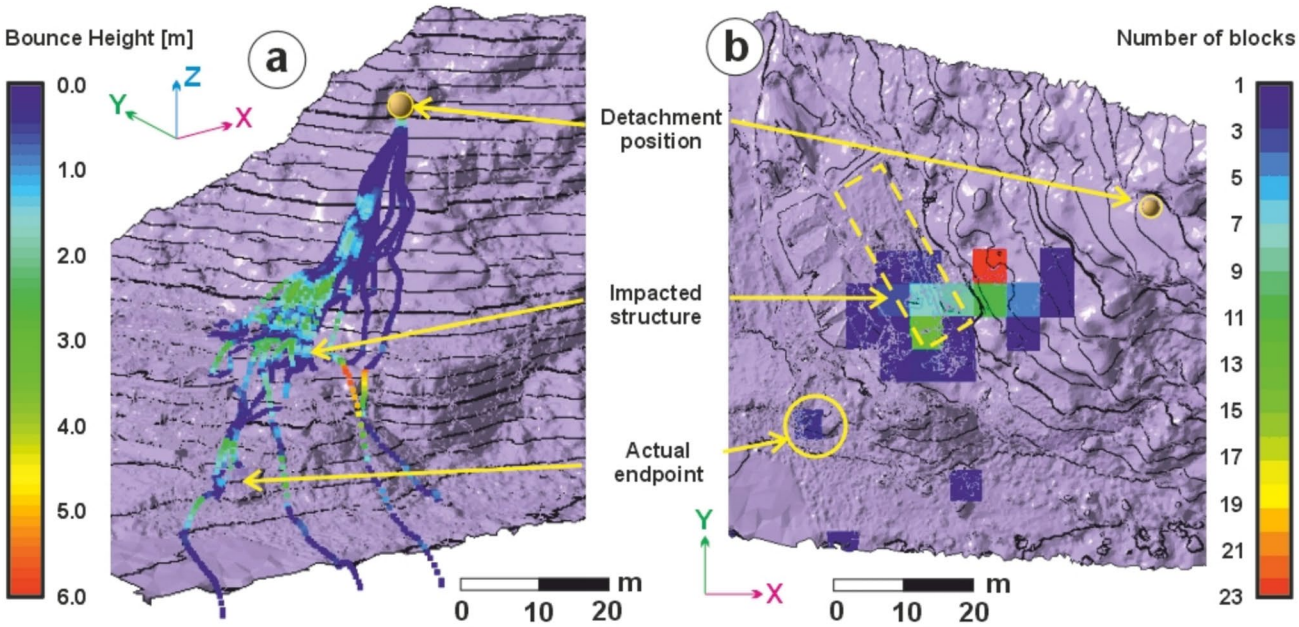

Fig. 10 RocFall3 simulation for Agia Fotia incident: **a**. Oblique 3D view of the trajectory paths and **b**. Spatial distribution on plan view of the trajectory endpoints (Topographic lines spacing is 2 m)

lation, the block impacts the building while airborne, with a total kinetic energy of more than 16,500 kJ.

iii. The trajectory endpoint calculated by RocFall3 coincides with the observed endpoint.

Kakia Skala rockfall incident

Kakia Skala setting

Kakia Skala (which translates to "bad staircase" in English) is an area prone to rockfalls documented even in Greek mythology. According to the work of Plutarch "The Parallel Lives – Theseus", Sciron, an Isthmian outlaw was located here and robbed and killed travelers by throwing rocks at them and forcing them over the cliffs and into the sea. Sciron was killed by Theseus, the king of Athens, in the same manner. Today, two of the tunnels in the area are named after Theseus and Sciron. Many minor rockfall incidents have been reported over the years in the area. However, limited detailed studies and publications are publicly available for the area regarding rockfalls. Mazarakis et al. (2021) presented the topographical, geological, tectonic and seismic features of the area, evaluated the rockfall hazard and proposed rockfall barriers to protect the highway.

Kakia Skala is defined by the south slope of mountain Kavallaris. The morphology is influenced by both alpine orogenesis structures and recent crust deformation. The predominant formation in the area is massive to thick-bedded limestone of white to sub-grey color of Middle-Upper Triassic age. Limestones are moderately weathered, but in places present high weathering and karstic erosion, mainly along the tectonic discontinuities. The area has been subjected to intense tectonic action of normal faults of East – West trending that run in parallel to the highway alignment and smaller transverse faults of direction (NW – SE) and is an active seismic zone (Rondoyanni and Marinos 2008).

3D model reconstruction

A full High Definition (1920 × 1080 pixels) UAV footage (https://www.youtube.com/watch?v=wMDbYSqzxRY) was released by Olympia Odos, the highway operator the day after the incident in YouTube® (youtube.com/@olympiaodos) and was broadly reproduced by Greek news media. Figure 12 presents the extracted video frame positions that were used in SfM method to reconstruct the terrain. The flight follows a linear pattern path, which is not ideal for the 3D reconstruction of non-corridor (e.g. roads) features such as this topographic terrain, but still can produce quality results within the overlapping area between the linear paths. To achieve high overlap (> 80%) between the image frames and considering the video playback speed, frames were extracted every 1 s. A total of 366 frames were extracted and processed.

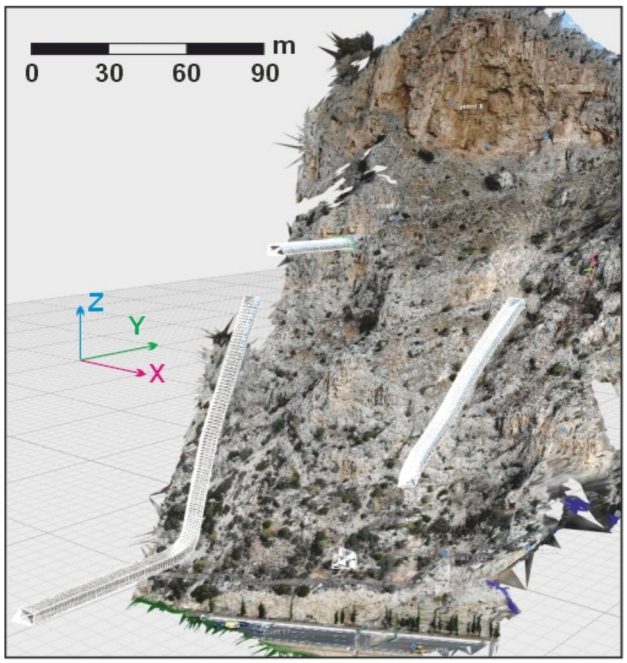

Fig. 12 Extracted video frames positions from UAV footage in 3D space over reconstructed 3D terrain for Kakia Skala site

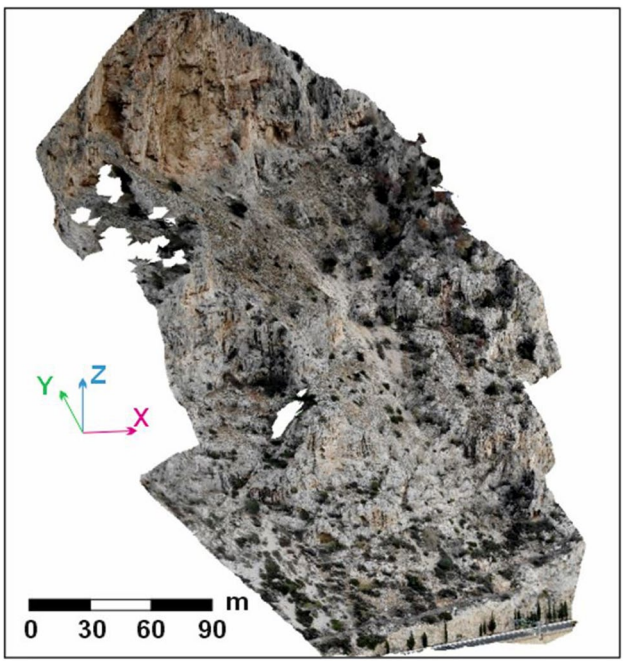

Fig. 13 Oblique view of the Kakia Skala 3D model. The highway is at the bottom right of the model

The 3D model covers an area of 0.4 km^2 (100 acres). Following the model scaling process, back-calculated flight height ranged between 50–150 m and the average ground resolution is calculated equal to 5 cm/pixel. The 3D model is shown in Fig. 13.

Evaluation of the 3D model

Similar to Agia Fotia case, the DTM model for this area from the Hellenic Cadastre was obtained. As mentioned earlier, the resolution of the Cadastre DTM model is 10 m, which is significantly lower than the 5 cm resolution of the UAV 3D model. The geometry of the terrain surface using the crowdsourced UAV footage visually resembles that of the Hellenic Cadastre DTM. Since this area is also small and the slope steep, the comparison between the 3D model and the Hellenic Cadastre DTM results in high RMS. Figure 14 presents this comparison with the color scale indicating the signed distance between the two models. Blue (negative values) indicates inwards distance, and red corresponds to outward distance. Due to the limited level of detail in the low resolution DTM of the Hellenic Cadastre, RMS equals to 73 cm and the standard deviation is 254 cm. Note that offset distances increase significantly at areas where the slope becomes vertical or negative. As the gradient becomes steeper, the topological features are considerably simplified when described by low resolution DTMs, increasing the projection error.

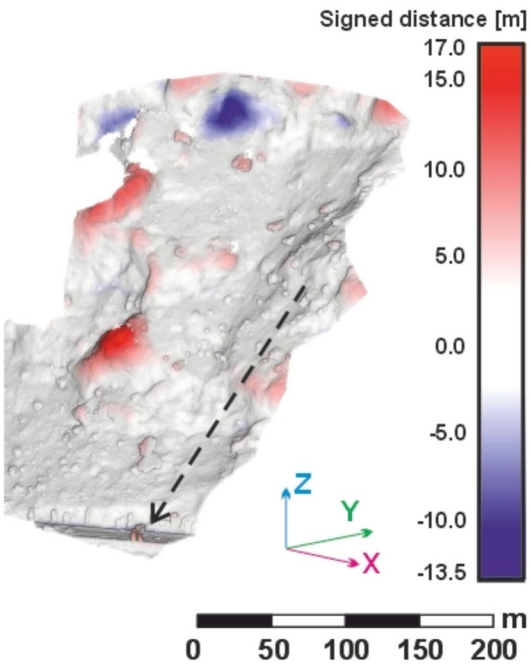

Fig. 14 Signed distance between the Hellenic Cadastre and the 3D model generated from the UAV. The dashed line shows the trajectory path. Blue (negative distances) indicates inward distance, and red corresponds to outward distance. The grey color covers 2 times the standard deviation ± 2.54 m

Rockfall assessment

The incident occurred on December 1st 2022. A number of rock blocks detached from approximately 150 m above road level (Fig. 15a), travelled on the slope that has a mean gradient of 65°, until they reached the highway (Fig. 15b). Two rockfall barriers intercepted the trajectories, but failed and allowed blocks to pass through (Fig. 15c), indicating that the energy at impact exceeded their capacity. However, the barriers were successful in reducing the energy of the block and during the subsequent impacts on the highway, limiting damage (Fig. 15d & e). Immediately after the incident the traffic was diverted to the Old National Road and restoration works began.

Since the area has minimal activity other than the highway traffic and the detachment zone is far upslope, no other crowdsourced images were found. The detachment position was determined by reviewing images of the slope before the incident in GoogleEarth and comparing them to the UAV footage.

The total volume of the debris at the road level was measured in the 3D model to be approximately 5 m^3 and the largest block was approximately equal to 1 m^3. However, the volume of the detached rock mass was reported to be significantly larger. In general, a block can fracture traveling downwards and some of the fragments may stop earlier resulting in lower volume at the endpoint. On the other hand, cases where a falling block causes disturbance and triggers the fall of other marginally stable blocks have been reported, resulting in larger volume at the endpoint. An example of that from Greece is the Tempi rockfall in 2008 (Christaras 2010).

Rockfall back-analysis through simulations

Trajectory analysis was performed with RocFall3 software using similar assumptions as for the back-analysis of Agia Fotia incident. The parameters selected to represent the limestone slope are presented in Table 1. The barriers are also simulated in the model, even though their properties could not be verified directly. The height of the barriers was measured from the 3D model to be equal to H = 2.5 m. Thus, we assumed that their capacity is E = 250 kJ, since barriers of that height usually belong to Energy Class 1 according to ETAG 027 Standard (Volkwein et al. 2019). In RocFall3 software, a block is stopped by the barrier provided that its kinetic energy is less than the barrier's capacity. If the block's kinetic energy is greater than the capacity of the barrier, then the block's energy is reduced by the barrier's capacity and continues its motion.

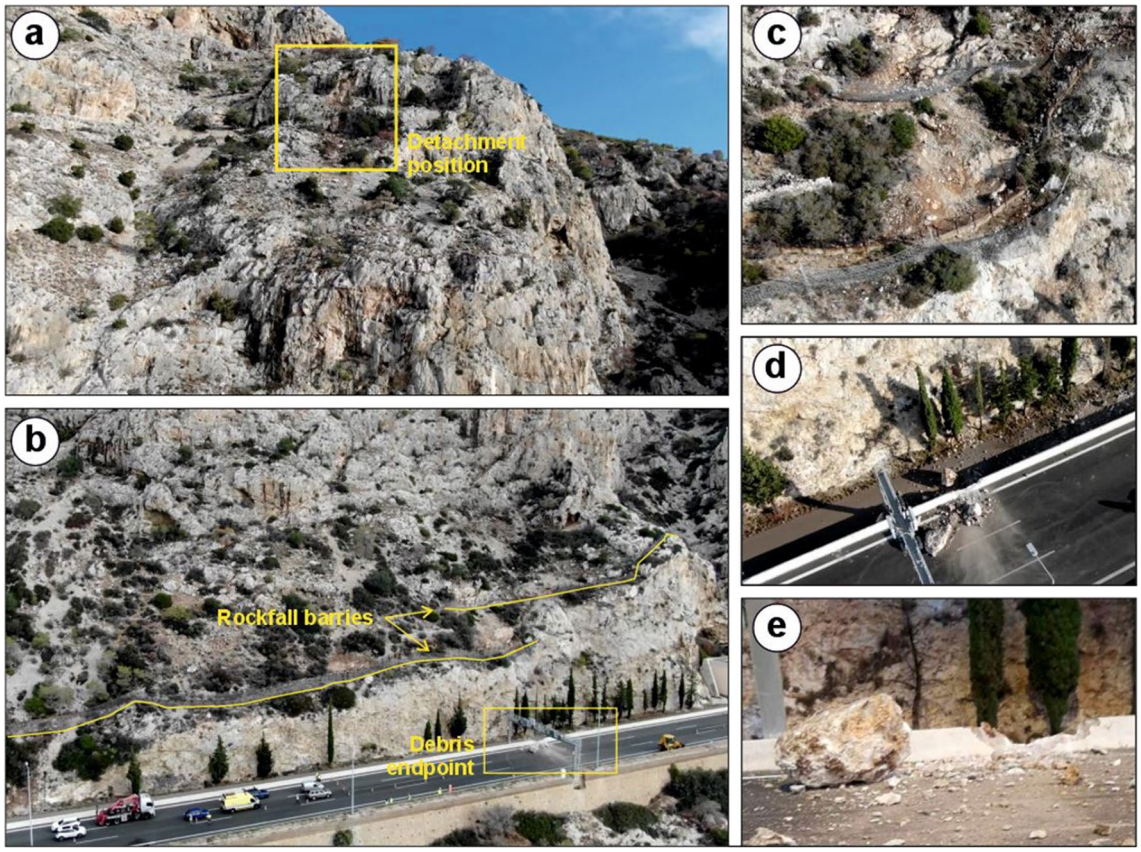

Fig. 15 Kakia Skala rockfall incident: **a**. detachment position; **b**. view of the highway and the position of the barriers; **c**. close view of the damaged barriers; **d**. and **e**. views of the trajectory endpoint at road level (all image frames are extracted from the UAV video, except e that was retrieved from protagon.gr)

The analysis is performed with a block mass equal to m = 2500 kg that corresponds to the largest block found on road level. This assumption leads to the least possible energy imposed on the barriers by that block, since it is highly probable that the block fractured prior to, or upon impact at, the road. A low initial translational velocity of 1 m/s oriented towards the slope's dip direction with an ± 30° offset was assigned to the block at the detachment position. A total of 100 blocks were released from the detachment position.

Figure 16a presents the trajectory paths as calculated by RocFall3 software, where the color indicates the bounce height. It is observed that approximately 10% of the blocks bounce over the top barrier and that 25% of the blocks penetrate it, meaning that the impact energy is higher than the barrier's capacity.

Figure 16b illustrates the spatial distribution of the trajectory endpoints. The barriers stop 70% of the simulated trajectories (60% at the top and 10% at the bottom barrier), 20% of the blocks stop at the road level and 10% travel beyond the 3D model's limits. Lateral dispersion is 28.8%, which is lower than its counterpart at the Agia Fotia site, but still higher than the range suggested by Azzoni and De Freitas (1995).

The closest match to the actual trajectory is illustrated in Fig. 17 superimposed on the digital model. The endpoint of this trajectory coincides with the deposition of the largest block on the road pavement. The block impacts the top barrier with an energy of 900 kJ and the bottom barrier with 740 kJ, that are considerably higher than the barriers capacity, causing their failure.

Discussion

Rockfall assessment with back-analysis in 3D space

Despite uncertainties associated with the size and fracturing of the falling blocks, the outcomes of the back-analyses reproduced the actual trajectories impressively well in both cases that were examined in this study. Compared to the effort required for similar back-analysis performed in two-dimensional space (Paronuzzi 2009; Saroglou et al.

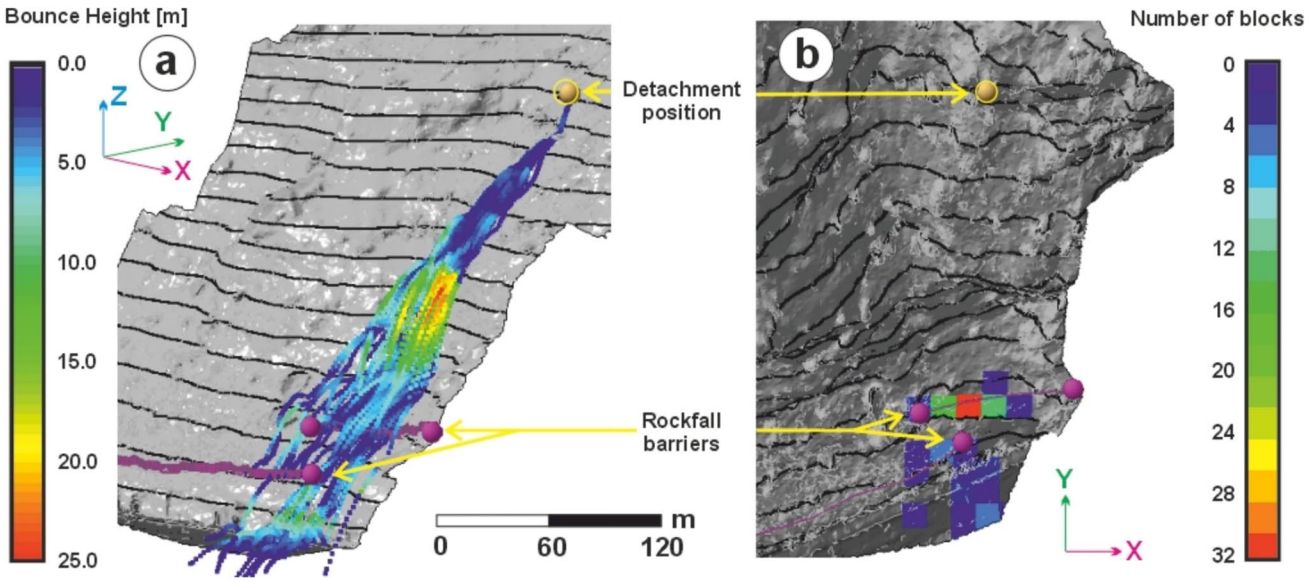

Fig. 16 RocFall3 simulation: **a**. Oblique view of trajectory paths and **b**. Spatial distribution on plan view of the trajectory endpoints (Topographic lines spacing is 10 m)

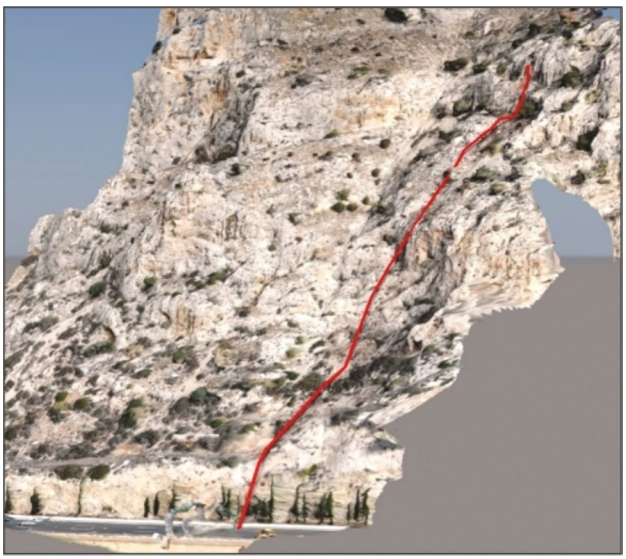

Fig. 17 Oblique view of the closest rockfall back-calculated trajectory from RocFall3 calculations superimposed on the digital model

2018), we observed that matching the actual trajectory required fewer trial-and-error attempts, and reduced modeling assumptions. This is attributed to the detailed terrain geometries that were generated and to the implementation of the motion analysis in the 3D dimensional space. This observation highlights the paramount importance of the 3D terrain geometry on the rockfall trajectories. Even though the importance of the 3rd dimension has been widely discussed in past research studies, it was commonly omitted due to the inherent additional challenges introduced in the analysis, particularly the ability to generate reliable 3D models in steep and inaccessible areas. The slope geometry, including the slope roughness are of great importance to the rockfall paths, the related variability and the deviation of the trajectories from the steepest gradient can be assessed only in a 3D space (Asteriou and Tsiambaos 2016; Azzoni et al. 1995; Bozzolo and Pamini 1986; Crosta and Agliardi 2004; Evans and Hungr 1993).

For the Agia Fotia incident, where the slope is convex, lateral dispersion was found to be considerable (equal to ~ 65%), while for the Kakia Skala incident, where the slope geometry is concave, lateral dispersion was ~ 29%. The observation that steeper slopes produce less dispersion (Azzoni and De Freitas 1995) is supported by this study, since in Kakia Skala the mean gradient is 65° while in Agia Fotia is 42°. However, in both cases lateral dispersion is higher than the range of 10–20% as suggested by Azzoni and De Freitas (1995). These findings demonstrate the importance of considering lateral dispersion in relevant design studies.

Benefits and limitations of the proposed approach

This study demonstrates that the proliferation of publicly available digital optical data, in this case UAV data collected by third parties, paired with technological innovations can facilitate the collection of valuable rockfall

incident data that can be back-analyzed fully remotely. The benefits of such an approach are:

i. the ability to generate accurate three-dimensional slope topography reconstruction inexpensively is paramount for the back-analysis of rockfalls, and can provide a better basis than topographic data available through nationwide resources (such as the Cadastre in this study);
ii. That high quality data for rockfall trajectory analysis collected within hours after an incident and posted online can be leveraged, even before any field deployment by geoprofessionals would be possible;
iii. perishable data (such as block sizes, fracturing, trajectory) is more likely to be preserved as restoration activities often start immediately after the incident and prior to any deployment by professionals;
iv. reliably leveraging third-party data may reduce or even eliminate the cost of field deployment and logistics involved, as well as enhance safety of individuals involved in data collection;
v. multiple on-line crowdsourced data may offer the opportunity to provide independent checks of the 3D models created and also validate the data used, or even possibly provide insights into earlier processes that may have occurred and gone unnoticed;
vi. analysis to understand the incident can start shortly after an incident, providing benefits in terms of time, the resources required for site deployment, and the scope of additional data collection;
vii. the back-analysis of the trajectory in 3D requires fewer assumptions and is more accurate compared to 2D modeling, as demonstrated from the two case studies presented in this paper.

However, there are also limitations associated with this approach. First, the availability of pre-incident optical footage (in this case UAV-based) is truly valuable for 3D model creation, comparison with a post-incident 3D model and volume differencing. Therefore, when pre-incident data is not available, less insights can be obtained. Still, this approach produces robust back-analysis results, as demonstrated in this work with Kakia Skala incident, where the trajectory back-analysis in 3D space was performed with less assumptions and proved to be superior to those obtained using typical methods in 2D space. The details of the footage associated with the flight path used by the UAV (which may not cover the area sufficiently to provide a detailed 3D model), the area coverage, the quality of footage available online (which may be lower in frames per second or resolution than the originally collected), may impact the 3D model creation. Permissions may be necessary for crowdsourced data that may be copyrighted or have terms of use depending on the hosting medium and the owner of the video. In general, it is permissible to use online resources for research under fair use principles. However, one must always check the specific terms and conditions that apply to the data they find to ensure legal compliance. The timing of the footage is also important to ensure that the pre-incident footage captures conditions that are representative prior to the incident. Finally, additional data is desired to assess the quality of the model, georeference it and make sure it is appropriate for reliable rockfall analyses.

Conclusions

This paper presents a fully remote approach to analyze rockfall incidents using exclusively crowdsourced optical data. The approach leverages data that becomes available immediately following an incident and includes information that is perishable, providing early insights on the incident that can also be useful for immediate restoration or other decisions. The steps are:

i. Datamine the internet for footage before and after an incident;
ii. Reconstruct the site morphology in three-dimensional space by applying the SfM method using crowdsourced optical footage (in this case UAV-based);
iii. Extract critical and perishable rockfall path and block size insights from the 3D model; and
iv. Conduct three-dimensional trajectory back-analysis using commercial rockfall software.

The approach is shown to work well, both in terms of 3D model acquisition and in terms of back-analysis of rockfall incidents. The 3D models created using crowdsourced data from different sources are consistent, and thus the process is reliable. Therefore, crowdsourced data can form the basis to back-analyze rockfall incidents.

Useful information to assess a rockfall can be extracted when a UAV footage before the incident is also available: the detachment position can be explicitly determined, the volume of the detached mass can be reliably calculated; the fragmentation of the block is detected; and the distribution of the fragments on the slope is determined. The latter is of great importance in the understanding of the mechanics involved during rockfalls.

Due to the complexity of the mechanisms that control the rockfall trajectory path and the paramount importance of the geometry of the slope, the evaluation of individual incidences is of limited value for generalized conclusions.

However, with the methodology described herein, past and future rockfall incidents can be analyzed in the three-dimensional space, with high precision for slope geometry. Data collected immediately after the event can form the basis for establishing a systematic, high accuracy and larger-than-previously possible inventory of motion characteristics from actual rockfall events. This is of value for generating more detailed and site-specific comparisons between simulations and reality that consider not just the initiation and final location of the rockfall but also the kinematics by matching the rockfall bounces, rolling and sliding sections. As a result, the reliability of the conclusions from the analyses increases and the insights affect positively associated risk assessment studies.

The work presented herein was based on online crowdsourced data. While this study focuses on rockfalls, the approach presented is not limited to them. Creating 3D models from crowdsourced data can be applied to other types of geohazards, such as landslides (as recently presented by An et al (2024)), debris flows, or even flood modeling. With the advanced analysis tools available today, having a reliable 3D model enables high-quality assessment, making this methodology broadly applicable to various geohazard scenarios. In addition, this approach can be used as a complement to any data collection deployment. Also, it can be implemented in various stages of a project, for example before the main exploration stage as an aid to better organize fieldwork. Depending on the acquisition time, the crowdsourced data may contain perishable information that might degrade significantly until field deployment.

The proposed approach holds substantial potential for international application, as it can be readily adapted to incidents across the globe where on-site visits may not be likely or possible. Moreover, this approach facilitates the collection of a diverse dataset that can support cross-regional comparisons and enhance understanding of destructive incidents across different geological and environmental contexts. This cumulative knowledge can ultimately inform international guidelines, improve predictive models, and contribute to the development of more effective mitigation strategies, making it a crucial advancement in the field of geohazard assessment.

Acknowledgements The authors acknowledge the contribution of Mr Giannis Avras and Mrs Foteini Asimakopoulou, senior year Geology students at the National and Kapodistrian University of Athens at the initial stages of this research, during their internship in Argo-E Group. The authors would like to thank Mr. Nikolaos Somarakis and Mr. Nikos Sarantos for granting permission to use their copyrighted UAV footages. Partial funding for the second author was provided by NASA under Grant No. 18-DISASTER18-0022.

Funding Open access funding provided by HEAL-Link Greece.

References

Agliardi F, Crosta GB, Frattini P (2009) Integrating rockfall risk assessment and countermeasure design by 3D modelling techniques. Nat Hazards Earth Syst Sci 9(4):1059–1073. https://doi.org/10.5194/nhess-9-1059-2009

An P, Yong R, Wang C, Jia S, Fang K (2024) Utilizing crowdsourced data for timely investigation of catastrophic landslide accidents: a case study of the coal mine collapse in inner Mongolia, China. Bull Eng Geol Env 83(9):354. https://doi.org/10.1007/s10064-024-03848-x

Asteriou P, Tsiambaos G (2016) Empirical model for predicting rockfall trajectory direction. Rock Mech Rock Eng 49:927–941. https://doi.org/10.1007/s00603-015-0798-7

Asteriou P, Tsiambaos G (2018) Effect of impact velocity, block mass and hardness on the coefficients of restitution for rockfall analysis. Int J Rock Mech Min Sci 106:41–50. https://doi.org/10.1016/j.ijrmms.2018.04.001

Asteriou P, Saroglou H, Tsiambaos G (2012) Geotechnical and kinematic parameters affecting the coefficients of restitution for rock fall analysis. Int J Rock Mech Min Sci 54:103–113. https://doi.org/10.1016/j.ijrmms.2012.05.029

Azzoni A, De Freitas M (1995) Experimentally gained parameters, decisive for rock fall analysis. Rock Mech Rock Eng 28(2):111–124. https://doi.org/10.1007/BF01020064

Azzoni A, La Barbera G, Zaninetti A (1995) Analysis and prediction of rockfalls using a mathematical model. International Journal of Rock Mechanics and Mining Sciences & Geomechanics Abstracts. https://doi.org/10.1016/0148-9062(95)00018-C

Bozzolo D, Pamini R (1986) Simulation of rock falls down a valley side. Acta Mech 63(1–4):113–130. https://doi.org/10.1007/BF01182543

Buzzi O, Giacomini A, Spadari M (2012) Laboratory investigation on high values of restitution coefficients. Rock Mech Rock Eng 45:35–43. https://doi.org/10.1007/s00603-011-0183-0

Carvajal-Ramírez F, Agüera-Vega F, Martínez-Carricondo PJ (2016). Effects of image orientation and ground control points distribution on unmanned aerial vehicle photogrammetry projects on a road cut slope. J Appl Remote Sens 10(3) https://doi.org/10.1117/1.JRS.10.034004

Chi E, Zhao M, Liu J, Kang Q (2015) Numerical modeling of rock fracture and fragmentation under impact loading using discrete element method. Adv Mech Eng 7(6):1687814015590295. https://doi.org/10.1177/1687814015590295

Christaras VPG, Vouvalidis K, Pavlides S (2010) Preliminary results regarding the rock falls of December 17 2009 at Tempi Greece.

Bulle Geol Soc Greece 43(3): 1122–1130 https://doi.org/10.12681/bgsg.11286
Cirillo D, Zappa M, Tangari AC, Brozzetti F, Ietto F (2024) Rockfall Analysis from UAV-Based Photogrammetry and 3D Models of a Cliff Area. Drones 8(1):31. https://doi.org/10.3390/drones8010031
Crosta G, Agliardi F (2004) Parametric evaluation of 3D dispersion of rockfall trajectories. Nat Hazard 4(4):583–598. https://doi.org/10.5194/nhess-4-583-2004
De Albuquerque JP, Herfort B, Brenning A, Zipf A (2015) A geographic approach for combining social media and authoritative data towards identifying useful information for disaster management. Int J Geogr Inf Sci 29(4):667–689. https://doi.org/10.1080/13658816.2014.996567
Dorren LK, Berger F (2006) Stem breakage of trees and energy dissipation during rockfall impacts. Tree Physiol 26(1):63–71. https://doi.org/10.1093/treephys/26.1.63
Evans S, Hungr O (1993) The assessment of rockfall hazard at the base of talus slopes. Can Geotech J 30(4):620–636. https://doi.org/10.1139/t93-054
Fanos AM, Pradhan B (2018) Laser scanning systems and techniques in rockfall source identification and risk assessment: a critical review. Earth Systems and Environment 2(2):163–182. https://doi.org/10.1007/s41748-018-0046-x
Farmakis I, DiFrancesco PM, Hutchinson DJ, Vlachopoulos N (2022) Rockfall detection using LiDAR and deep learning. Eng Geol 309:106836. https://doi.org/10.1016/j.enggeo.2022.106836
Giacomini A, Thoeni K, Lambert C, Booth S, Sloan S (2012) Experimental study on rockfall drapery systems for open pit highwalls. Int J Rock Mech Min Sci 56:171–181. https://doi.org/10.1016/j.ijrmms.2012.07.030
Grady CL, Santi PM, Walton G, Luza C, Salas G, Meza P, Riega SPC (2024) A Remote-Sensing-Based Method Using Rockfall Inventories for Hazard Mapping at the Community Scale in the Arequipa Region of Peru. Remote Sensing 16(19):3732. https://doi.org/10.3390/rs16193732
Guzzetti F, Reichenbach P, Ghigi S (2004) Rockfall hazard and risk assessment along a transportation corridor in the Nera Valley. Central Italy Environmental Management 34(2):191–208. https://doi.org/10.1007/s00267-003-0021-6
Hao W, Jian H, Xiang H, Jingqing Y, Zicheng H, Ying H (2021) A New Rockfall Simulation Tool based on Unity 3D. IOP Conference Series: Earth and Environmental Science. https://doi.org/10.1088/1755-1315/861/3/032059
Harrap R, Hutchinson D, Sala Z, Ondercin M, Difrancesco PM (2019) Our GIS is a game engine: Bringing Unity to spatial simulation of rockfalls. *GeoComputation 2019*, 11–14. https://doi.org/10.17608/K6.AUCKLAND.9848612.V2
Heidenreich B (2004) Small-and half-scale experimental studies of rockfall impacts on sandy slopes. PhD Thesis, EPFL - Switzerland
Hoek E (1987) Rockfall-A program in Basic for the analysis of rockfalls from slopes. Unpublished note, Golder Associates/University of Toronto, Canada
Jaud M, Le Dantec N, Parker K, Lemon K, Lendre S, Delacourt C, Gomes RC (2022) How to Include Crowd-Sourced Photogrammetry in a Geohazard Observatory—Case Study of the Giant's Causeway Coastal Cliffs. Remote Sensing 14(14):3243. https://doi.org/10.3390/rs14143243
Kakavas MP, Nikolakopoulos KG (2021) Digital Elevation Models of Rockfalls and Landslides: A Review and Meta-Analysis. Geosciences 11(6):256. https://doi.org/10.3390/geosciences11060256
Labiouse V, Heidenreich B (2009) Half-scale experimental study of rockfall impacts on sandy slopes. Nat Hazard 9(6):1981–1993. https://doi.org/10.5194/nhess-9-1981-2009
Ma K, Liu G, Xu N, Zhang Z, Feng B (2021) Motion characteristics of rockfall by combining field experiments and 3D discontinuous deformation analysis. Int J Rock Mech Min Sci 138:104591. https://doi.org/10.1016/j.ijrmms.2020.104591
Manousakis J, Zekkos D, Saroglou F, Clark M (2016) Comparison of UAV-enabled photogrammetry-based 3D point clouds and interpolated DSMs of sloping terrain for rockfall hazard analysis. Int Arch Photogramm Remote Sens Spat Inf Sci 42:71–77. https://doi.org/10.5194/isprs-archives-XLII-2-W2-71-2016
Mazarakis K, Diamantis K, Fereidooni D (2021) Rockfall analysis in the area of Kakia Skala, Greece. Arab J Geosci 14:1–15. https://doi.org/10.1007/s12517-021-07307-9
Moos C, Dorren L, Stoffel M (2017) Quantifying the effect of forests on frequency and intensity of rockfalls. Nat Hazard 17(2):291–304. https://doi.org/10.5194/nhess-17-291-2017
Noël F, Nordang SF, Jaboyedoff M, Travelletti J, Matasci B, Digout M, Derron MH, Caviezel A, Hibert C, Toe D (2023) Highly energetic rockfalls: back analysis of the 2015 event from the Mel de la Niva. Switzerland Landslides 20(8):1561–1582. https://doi.org/10.1007/s10346-023-02054-2
Obda O, El Kharim Y, Obda I, Ahniche M, El Kouffi A (2024) Coastal rocky slopes instability analysis and landslide frequency-area distribution alongside the road network in west Mediterranean context (Northern of Morocco). Nat Hazards 120(4):3401–3428. https://doi.org/10.1007/s11069-023-06342-x
Ondercin M (2016) An Exploration of rockfall modelling through game engines. MSc Thesis, Queen's University, Canada
Papastamatiou J, Vetoulis D, Tataris A (1959) *Geological map of Greece: Ierapetra sheet*. Institute for Geology and Subsurface Research.
Paronuzzi P (2009) Field evidence and kinematical back-analysis of block rebounds: the lavone rockfall, Northern Italy. Rock Mech Rock Eng 42:783–813. https://doi.org/10.1007/s00603-008-0021-1
Pfeiffer TJ, Bowen TD (1989) Computer simulation of rockfalls. Bull Assoc Eng Geol 26(1):135–146. https://doi.org/10.2113/gseegeosci.xxvi.1.135
Pierson LA (1991) The rockfall hazard rating system. (No. FHWA-OR-GT-92–05). Oregon State Highway Division. Engineering Geology Group.
Prades-Valls A, Corominas J, Lantada N, Matas G, Núñez-Andrés MA (2022) Capturing rockfall kinematic and fragmentation parameters using high-speed camera system. Eng Geol 302:106629. https://doi.org/10.1016/j.enggeo.2022.106629
RocScience (2022) RocFall3 Manual
Rondoyanni T, Marinos P (2008) The Athens-Corinth highway and railway crossing a tectonically active area in Greece. Bull Eng Geol Env 67:259–266. https://doi.org/10.1007/s10064-008-0134-5
Sala Z, Hutchinson DJ, Harrap R (2019) Simulation of fragmental rockfalls detected using terrestrial laser scans from rock slopes in south-central British Columbia, Canada. Nat Hazard 19(11):2385–2404. https://doi.org/10.5194/nhess-19-2385-2019
Saroglou H, Marinos V, Marinos P, Tsiambaos G (2012) Rockfall hazard and risk assessment: an example from a high promontory at the historical site of Monemvasia, Greece. Nat Hazard 12(6):1823–1836. https://doi.org/10.5194/nhess-12-1823-2012
Saroglou C, Asteriou P, Tsiambaos G, Zekkos D, Clark M, Manousakis J (2017) Investigation of two co-seismic rockfalls during the 2015 Lefkada and 2014 Cephalonia earthquakes in Greece. Proceedings of the 3rd North American Symposium on Landslides, Roanoke, VA, USA,
Saroglou C, Asteriou P, Zekkos D, Tsiambaos G, Clark M, Manousakis J (2018) UAV-based mapping, back analysis and

trajectory modeling of a coseismic rockfall in Lefkada island, Greece. Nat Hazard 18(1):321–333. https://doi.org/10.5194/nhess-18-321-2018

Šašak J, Gallay M, Kaňuk J, Hofierka J, Minár J (2019) Combined Use of Terrestrial Laser Scanning and UAV Photogrammetry in Mapping Alpine Terrain. Remote Sensing 11(18):2154. https://doi.org/10.3390/rs11182154

Spadari M, Giacomini A, Buzzi O, Fityus S, Giani G (2012) In situ rockfall testing in New South Wales, Australia. Int J Rock Mech Min Sci 49:84–93. https://doi.org/10.1016/j.ijrmms.2011.11.013

Stumpf A, Malet JP, Kerle N, Niethammer U, Rothmund S (2013) Image-based mapping of surface fissures for the investigation of landslide dynamics. Geomorphology 186:12–27. https://doi.org/10.1016/j.geomorph.2012.12.010

Volkwein A, Gerber W, Klette J, Spescha G (2019) Review of approval of flexible rockfall protection systems according to ETAG 027. Geosciences 9(1):49. https://doi.org/10.3390/geosciences9010049

Wang Y, Tonon F (2011) Discrete element modeling of rock fragmentation upon impact in rock fall analysis. Rock Mech Rock Eng 44:23–35. https://doi.org/10.1007/s00603-010-0110-9

Wang X, Frattini P, Crosta G, Zhang L, Agliardi F, Lari S, Yang Z (2014) Uncertainty assessment in quantitative rockfall risk assessment. Landslides 11:711–722. https://doi.org/10.1007/s10346-013-0447-8

Westoby MJ, Brasington J, Glasser NF, Hambrey MJ, Reynolds JM (2012) 'Structure-from-Motion'photogrammetry: A low-cost, effective tool for geoscience applications. Geomorphology 179:300–314. https://doi.org/10.1016/j.geomorph.2012.08.021

Yu M, Yang C, Li Y (2018) Big data in natural disaster management: a review. Geosciences 8(5):165. https://doi.org/10.3390/geosciences8050165

Žabota B, Kobal M (2020) A new methodology for mapping past rockfall events: From mobile crowdsourcing to rockfall simulation validation. ISPRS Int J Geo Inf 9(9):514. https://doi.org/10.3390/ijgi9090514

Zekkos D, Greenwood W, Lynch J, Manousakis J, Athanasopoulos-Zekkos A, Clark M, Saroglou C (2018) Lessons learned from the application of UAV-enabled structure-from-motion photogrammetry in geotechnical engineering. International Journal of Geoengineering Case Histories 4(4):254–274. https://doi.org/10.4417/IJGCH-04-04-03

Zekkos D, Tsavalas-Hardy A, Mandilaras G, Tsantilas K (2019) Using social media to assess earthquake impact on people and infrastructure: Examples from earthquakes in 2018. Proc. 2nd Int. Conf. Natural Hazards Infrastructure,

Zhao T, Crosta GB, Utili S, De Blasio FV (2017) Investigation of rock fragmentation during rockfalls and rock avalanches via 3-D discrete element analyses. J Geophys Res Earth Surf 122(3):678–695. https://doi.org/10.1002/2016JF004060